OXFORD

Human Molecular Genetics, 2017, Vol. 26, No. 20 3935–3945

doi: 10.1093/hmg/ddx281
Advance Access Publication Date: 17 July 2017
Original Article

ORIGINAL ARTICLE

Potassium channel dysfunction underlies Purkinje neuron spiking abnormalities in spinocerebellar ataxia type 2

James M. Dell'Orco[1], Stefan M. Pulst[2] and Vikram G. Shakkottai[1,3,*]

[1]Department of Neurology, University of Michigan Medical School, Ann Arbor, MI 48103, USA, [2]Department of Neurology, University of Utah, Salt Lake City, UT 84112, USA and [3]Department of Molecular and Integrative Physiology, University of Michigan, Ann Arbor, MI 48109, USA

*To whom correspondence should be addressed at: Department of Neurology, University of Michigan, 4009 BSRB, 109 Zina Pitcher Place, Ann Arbor, MI 48109, USA. Tel: 734 6156891; Fax: 734 6479777; Email: vikramsh@med.umich.edu

Abstract

Alterations in Purkinje neuron firing often accompany ataxia, but the molecular basis for these changes is poorly understood. In a mouse model of spinocerebellar ataxia type 2 (SCA2), a progressive reduction in Purkinje neuron firing frequency accompanies cell atrophy. We investigated the basis for altered Purkinje neuron firing in SCA2. A reduction in the expression of large-conductance calcium-activated potassium (BK) channels and Kv3.3 voltage-gated potassium channels accompanies the inability of Purkinje neurons early in disease to maintain repetitive spiking. In association with prominent Purkinje neuron atrophy, repetitive spiking is restored, although at a greatly reduced firing frequency. In spite of a continued impairment in spike repolarization and a persistently reduced BK channel mediated afterhyperpolarization (AHP), repetitive spiking is maintained, through the increased activity of barium-sensitive potassium channels, most consistent with inwardly rectifying potassium (K_{ir}) channels. Increased activity of K_{ir} channels results in the generation of a novel AHP not seen in wild-type Purkinje neurons that also accounts for the reduced firing frequency late in disease. Homeostatic changes in Purkinje neuron morphology that help to preserve repetitive spiking can also therefore have deleterious consequences for spike frequency. These results suggest that the basis for spiking abnormalities in SCA2 differ depending on disease stage, and interventions targeted towards correcting potassium channel dysfunction in ataxia need to be tailored to the specific stage in the degenerative process.

Introduction

Purkinje neurons exhibit autonomous firing in the absence of synaptic input (1). The spontaneous firing of Purkinje neurons is normally extremely precise, with nearly uniform interspike interval duration (2). Modulation of Purkinje neuron intrinsic firing by synaptic input shapes the precision of movement (3–5). Disruption of Purkinje neuron spiking is associated with cerebellar ataxia (6,7). Spinocerebellar ataxias (SCAs) constitute a group of dominantly inherited neurodegenerative disorders with involvement of the cerebellum and its associated pathways (8). Neuronal dysfunction precedes neuronal loss in mouse models of SCA. A shared pattern of neuronal dysfunction in different mouse models of SCA, includes a progressive reduction in cerebellar Purkinje neuron firing frequency. A reduction in Purkinje neuron firing frequency is seen in mouse models of SCA1 (9,10), SCA2 (11), SCA3 (12), SCA5 (13), and SCA27 (14). In a mouse model of SCA2 there is a correlation between reduced spike frequency, motor impairment and progressive thinning of

Received: April 21, 2017. **Revised:** July 10, 2017. **Accepted:** July 13, 2017

the cerebellar molecular layer, a surrogate for Purkinje neuron dendritic atrophy (11).

Autonomous spiking in Purkinje neurons relies on the interplay between a number of ion channels (1). The depolarization during the upstroke of the action potential is mediated primarily by the voltage-gated sodium channel, Nav1.6. Action potential repolarization is mediated by voltage-gated potassium channels, including Kv3.3 (15). Importantly, in order to maintain autonomous repetitive spiking, there is critical need for large conductance calcium-activated (BK) and small conductance calcium-activated (SK) potassium channels responsible for the afterhyperpolarization (AHP) (16–18). Alterations in spiking in SCAs may be attributed to specific changes in ion channel expression and function. In a mouse model of SCA3, changes in firing were attributed to altered function of Kv1 potassium channels (12). In SCA27 reduced function of the voltage-gated sodium channel, Nav1.6, is associated with the reduced Purkinje neuron firing (14). In SCA1, these changes in firing are due to a reduction in expression and function of BK and G-protein coupled inwardly rectifying potassium (GIRK) channels (10). Although changes in firing described in SCA1 are present in SCA2 Purkinje neurons (11), the basis for these changes in firing remain unexplained.

Here we demonstrate that reduced expression of Kv3.3 and BK channels accompanies the reduction in firing frequency in SCA2 Purkinje neurons. In spite of reduced BK channel expression, BK channel function continues to be necessary for repetitive spiking. The reduced firing frequency at a disease stage when there is significant Purkinje neuron atrophy, is however, not directly due to reduced Kv3.3 and BK expression, but the development of a novel AHP with slow kinetics.

Results

Alterations in firing in cerebellar Purkinje neurons in the ATXN2[127Q] model of SCA2 result from a reduction in potassium channel transcripts

In the ATXN2[127Q] model of SCA2, a progressive reduction in cerebellar Purkinje neuron firing frequency occurs in association with dendritic degeneration (11). At the outset of dendritic degeneration at 12 weeks, firing frequency is modestly reduced, but is markedly reduced by 24 weeks. Cell loss is not evident until 40 weeks (11). The basis for the changes in Purkinje neuron firing in this model of SCA2 are not clear. We wished to determine the basis for changes in Purkinje neuron firing at 12 and 25 weeks, prior to the onset of significant cell loss. At 12 weeks, in cell attached recordings from cerebellar slices, wild-type Purkinje neurons uniformly exhibited repetitive spiking (Fig. 1A and C). Surprisingly, over 55% of Purkinje neurons from ATXN2[127Q] littermates displayed no evidence of spiking (Fig. 1B and C). The ∼45% of ATXN2[127Q] neurons that did display repetitive spiking had a lower firing frequency (Fig. 1D). The modest reduction in firing frequency is consistent with a prior study using extracellular cerebellar slice recordings in these mice (11). In order to determine the basis for a lack of spiking, and an overall reduction in firing frequency ATXN2[127Q] Purkinje neurons, we performed whole-cell patch-clamp recordings. Wild-type neurons continued to display regular repetitive spiking (Fig. 1E). Purkinje neurons from ATXN2[127Q] mice that did not display repetitive spiking in the cell attached configuration, also did not display repetitive spiking in the whole-cell configuration. These non-firing cells had a relatively depolarized membrane potential (Fig. 1F).

In order to determine the basis for the lack of spiking in depolarized ATXN2[127Q] Purkinje neurons, in whole-cell configuration, cells were hyperpolarized to −90 mV, and depolarized with sequentially increasing current injection. ATXN2[127Q] Purkinje neurons were capable of generating spikes, but were unable to sustain spike trains for the duration of the step for more than a few current steps (Fig. 2A), unlike wild-type littermate controls that could sustain spike trains for entire duration of the current step with injected current (Fig. 2B). With lower levels of injected current compared to wild-type neurons, action potentials trains in ATXN2[127Q] Purkinje neurons underwent a plateau potential (Fig. 2C), consistent with depolarization block of repetitive spiking, a phenomenon we previously described in models of SCA1 (10) and SCA3 (12). The three-fold lower threshold to depolarization block was only explained in part by ∼1.5-fold increase in input resistance in ATXN2[127Q] Purkinje neurons (Supplementary Material, Fig. S1A and B). We therefore also examined characteristics of action potentials evoked from a negative holding potential of −90 mV in order to determine the basis for inability of ATXN2[127Q] Purkinje to sustain spike trains. In spite of the action potential threshold being more depolarized in ATXN2[127Q] Purkinje neurons (Supplementary Material, Fig. S1C), spike height was not impaired (Supplementary Material, Fig. 1D). Corresponding to the more depolarized action potential threshold, the maximal slope of the rising phase of the action potential was reduced in ATXN2[127Q] Purkinje neurons (Supplementary Material, Fig. S1E). These data suggest a functional impairment in voltage-gated sodium channels, but do not explain either depolarization block of repetitive spiking or the depolarized membrane potential of ATXN2[127Q] Purkinje neurons. Since depolarization block of repetitive spiking is associated with reduced potassium channel function (10,12), we determined whether spike repolarization and the AHP, both mediated by potassium channels, were impaired. The amplitude of the AHP measured from the spike threshold (Fig. 2D and E) as well as the maximal slope of the repolarization phase of the action potential (Fig. 2F) were significantly impaired. Since the action potential threshold is significantly more depolarized in ATXN2[127Q] Purkinje neurons, and this may confound the measurement of the AHP, the absolute value of the AHP from the peak was also measured (Fig. 2G). The AHP was more depolarized in ATXN2[127Q] Purkinje neurons. We also measured the AHP and the time to the AHP minimum from the peak of the action potential, using short 10 ms depolarizing steps from −90 mV. The AHP amplitude was reduced, and the time to AHP minimum was similar in wild-type and ATXN2[127Q] Purkinje neurons (Fig. 2H–J). These data are consistent with impaired repolarizing potassium conductances in ATXN2[127Q] Purkinje neurons.

In order to determine the underlying molecular basis for these changes in potassium channel function, we looked at transcript levels of potassium channels important for Purkinje neuron spiking. Cerebellar RNA sequencing data from these mice (19) showed a reduction in transcript levels of BK channels (gene: *Kcnma1*), important for the AHP (18) as well as Kv3.3 (gene: *Kcnc3*) and Kv3.1 (gene: *Kcnc1*) channels, important for spike repolarization (15) (Fig. 3A). Other potassium channels, including SK channels showed no reduction in transcript levels (not shown). Progressive changes in BK (Fig. 3B) and Kv3.3 (Fig. 3C) expression were confirmed by quantitative RT-PCR from whole-cerebellar lysates. Immunostaining for BK channels, with an antibody that has been validated in knockout mice (20) confirmed a reduction in BK channel expression in ATXN2[127Q] Purkinje neurons (Fig. 3D–J).

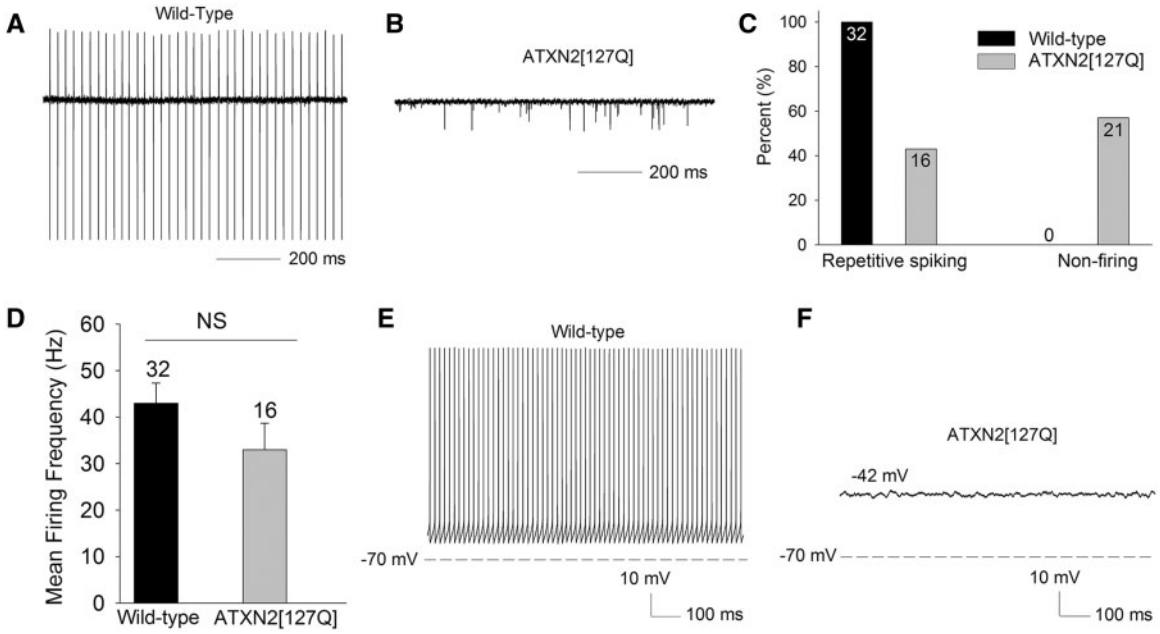

Figure 1. ATXN2[127Q] Purkinje neurons exhibit impaired spiking at 12 weeks. (**A**) Wild-type Purkinje neurons exhibit repetitive spiking (**B**) A significant proportion of ATXN2[127Q] Purkinje neurons lack spiking at 12 weeks, summarized in (**C**). (**D**) The firing frequency of firing ATXN2[127Q] Purkinje neurons is not statistically significantly reduced at this time point. (**E**) In the whole-cell configuration wild-type Purkinje neurons continue to display regular, repetitive spiking. (**F**) Non-firing ATXN2[127Q] Purkinje neurons display a depolarized membrane potential. Data were analysed with a Student's *t*-test, and are displayed as mean ± SEM.

These data suggest that at 12 weeks, the reduction in firing frequency, and the loss of spiking in a subset of ATXN2[127Q] Purkinje neurons is associated with the reduction in expression and function of BK and Kv3 channels.

Preservation of spiking in 25-week atrophic ATXN2[127Q] Purkinje neurons is associated with a normal AHP amplitude

Later in disease, at 25 weeks, ATXN2[127Q] Purkinje neurons undergo marked cell atrophy (11). In order to confirm the previously reported reduction in Purkinje neuron firing frequency this stage in disease when there is marked Purkinje neuron dendritic degeneration, but no cell loss (11), we performed cell-attached recordings from 25-week-old ATXN2[127Q] Purkinje neurons. Wild-type neurons display repetitive firing (Fig. 4A) with a firing frequency that is similar to that seen at 12 weeks (Fig. 4A and C). 25-week-old ATXN2[127Q] Purkinje neurons uniformly exhibited repetitive spiking, but at a markedly reduced firing frequency (Fig. 4B and C). In order to determine whether the reduced firing frequency in ATXN2[127Q] Purkinje neurons, was due to altered synaptic activity, we performed cell-attached recordings in the absence and then presence of 50 μM picrotoxin and 5 μM DNQX to block inhibitory and excitatory synaptic transmission. The firing frequency of ATXN2[127Q] Purkinje neurons was unchanged in the presence of synaptic inhibitors (18.7 ± 7.0 Hz before, and 20.7 ± 5.2 Hz in the presence of synaptic inhibitors, $n = 6$, $P = 0.482$), consistent with our prior studies suggesting that there is little tonic synaptic activity on Purkinje neurons in acute cerebellar slices (10,12). In order to determine the changes in intrinsic membrane excitability that accounts for the reduction in firing, we performed whole-cell recordings. Wild-type neurons continued to exhibit repetitive spiking (Fig. 4D), as did ATXN2[127Q] Purkinje neurons (Fig. 4E). Following an action potential, the membrane potential hyperpolarizes to values more negative than the spike threshold. The most negative value of this post-spike hyperpolarization defines the afterhyperpolarization (AHP). Unlike in 12-week-old ATXN2[127Q] Purkinje neurons, however, at 25 weeks these neurons had an AHP that achieved the same amplitude as in wild-type littermate controls (Fig. 4F). In order to also directly compare the amplitude of the AHP between 12 and 25-week ATXN2[127Q] Purkinje neurons, we evoked spikes after holding the membrane potential at −90 mV in 25-week ATXN2[127Q] Purkinje neurons. The amplitude of the AHP in evoked spikes was similar to spontaneous spikes in 25-week ATXN2[127Q] Purkinje neurons and significantly more negative as compared to the AHP of 12-week ATXN2[127Q] Purkinje neurons (AHP minimum −66.5 ± 1.0 mV, $n = 9$, $P < 0.001$ compared to the AHP in ATXN2[127Q] Purkinje neurons at 12 weeks as seen in Fig. 2H and I). These results suggest that the restoration of spiking in ATXN2[127Q] Purkinje neurons is associated with their ability to now generate an AHP of normal amplitude.

Impairments of BK and Kv3.3 function continue to be present in 25-week atrophic ATXN2[127Q] Purkinje neurons

In SCA1 mice, in spite of a progressive reduction in BK channel transcript levels with cell atrophy, an increase in density of BK channels due to Purkinje neuron atrophy helps these channels maintain a normal AHP amplitude (10). We wished to examine whether atrophy plays a similar homeostatic role to preserve BK and Kv3.3 channel function, in spite of reduced transcript levels, in ATXN2[127Q] mice. Although the amplitude of the AHP was similar in ATXN2[127Q] Purkinje neurons and littermate wild-type controls (Figs 4F and 5A), we wished to examine the component of the AHP mediated by BK channels. BK channels normally contribute maximally to the component of the AHP that closely follows, and is within 1 ms of the peak of the spike (so called "fast-AHP") (18). In wild-type neurons the fast-

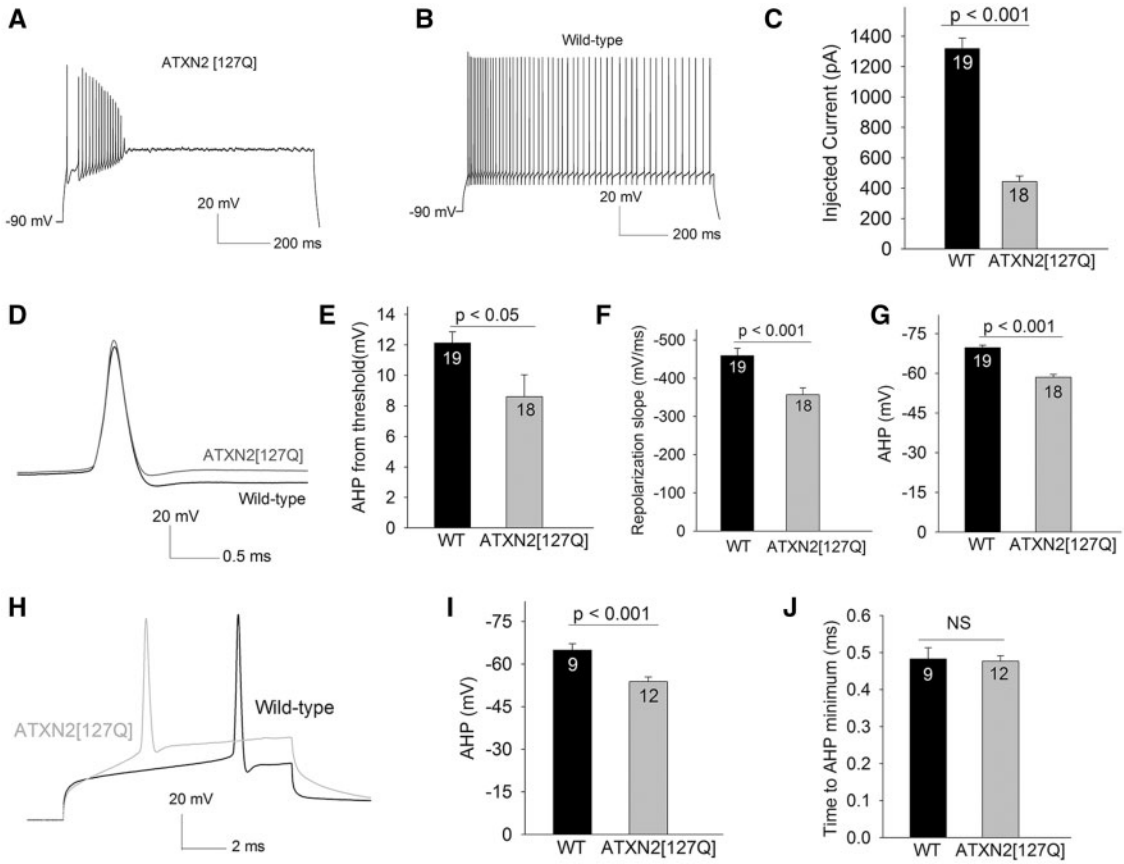

Figure 2. Impaired spiking in 12-week ATXN2[127Q] Purkinje neurons is secondary to loss of repolarizing potassium conductances. (**A**) In response to depolarizing current injection of 650 pA from a negative holding potential of −90 mV, ATXN2[127Q] Purkinje neurons can generate spikes, but cannot sustain spike trains. (**B**) Purkinje neurons from wild-type littermate controls can sustain high rates of repetitive firing in response to the same amount of depolarizing current injection. (**C**) The amount of injected current needed for ATXN2[127Q] Purkinje neurons to undergo depolarization block of repetitive spiking is significantly lower than in wild-type littermate controls. (**D**) The inability of ATXN2[127Q] Purkinje neurons to sustain spike trains is associated with slower spike repolarization and a reduction the amplitude of the AHP. For clarity, traces with similar spike threshold in ATXN2[127Q] and wild-type Purkinje neurons are shown. (**E**) Summary of AHP amplitude from threshold. (**F**) Summary of spike repolarization slope. (**G**) The absolute value of the AHP is more depolarized in ATXN2[127Q] Purkinje neurons. (**H**) Single spikes were evoked using 10 ms depolarizing steps from −90 mV. Note the reduction in AHP amplitude in ATXN2[127Q] Purkinje neurons, without a change in spike height or the time to minimum AHP, summarized in (**I, J**) Numbers within the bars indicate numbers of cells. Data were analysed with a Student's *t*-test, and are displayed as mean ± SEM.

AHP closely corresponded to the AHP minimum (Compare Figs 4F, 5C and D, $P = 0.35$), confirming that the AHP is mediated primarily by BK channels. In marked contrast in ATXN2[127Q] Purkinje neurons, the fast-AHP amplitude was significantly reduced (Fig. 5C and D), in spite of a normal overall AHP amplitude (Fig. 4F and 5A). The AHP minimum in ATXN2[127Q] Purkinje neurons was also significantly delayed (Fig. 5E), suggesting that it is generated by a current distinct from BK channels. Since the AHP is sensitive to calcium buffering, and expression of calbindin, a major calcium buffer in Purkinje neurons is reduced in ATXN2[127Q] Purkinje neurons (11), measurement of the AHP at this age with the same calcium buffer as for wild-type mice may underestimate the function of BK channels. To address this possibility, patch-clamp recordings were performed in the cell-attached followed by the whole-cell configuration. The firing frequency and regularity of spiking as represented by the coefficient of variation (CV) were indistinguishable between the whole-cell and cell-attached configuration (Frequency and CV cell attached: 9.3 ± 1.9 Hz, 0.091 ± 0.02; Frequency and CV whole cell: 12.3 ± 2.4 Hz, 0.09± 0.01, $n = 9$), suggesting that in spite of a reduction in transcripts for calcium buffering proteins, buffering capacity is not significantly altered in 25-week-old ATXN2[127Q] Purkinje neurons. Spike repolarization, mediated by Kv3.3 channels (15), continued to be impaired in 25-week-old ATXN2[127Q] Purkinje neurons (Figs 2D and F, 5A and F). These results suggest that Purkinje neuron atrophy is unable to compensate for the loss of BK and Kv3.3 channels in ATXN2[127Q] mice. Reduced transcript levels of these channels are associated with continued functional impairment in both BK and Kv3.3 channels. ATXN2[127Q] Purkinje neurons are nevertheless able to maintain pacemaker firing due to the presence of an AHP that has novel kinetic properties.

BK channels continue to play an important role in generating discrete spikes in 25-week atrophic ATXN2[127Q] Purkinje neurons

We wished to determine the molecular basis for the novel AHP associated with slowed firing frequency in ATXN2[127Q] Purkinje neurons. In order to first determine whether assumption of novel kinetic properties by BK channels could explain this AHP. The AHP in Purkinje neurons is normally mediated by calcium-activated potassium channels. In order to determine the role that BK channels play in spiking in 25-week-old ATXN2[127Q] Purkinje neurons, we first determined the role of

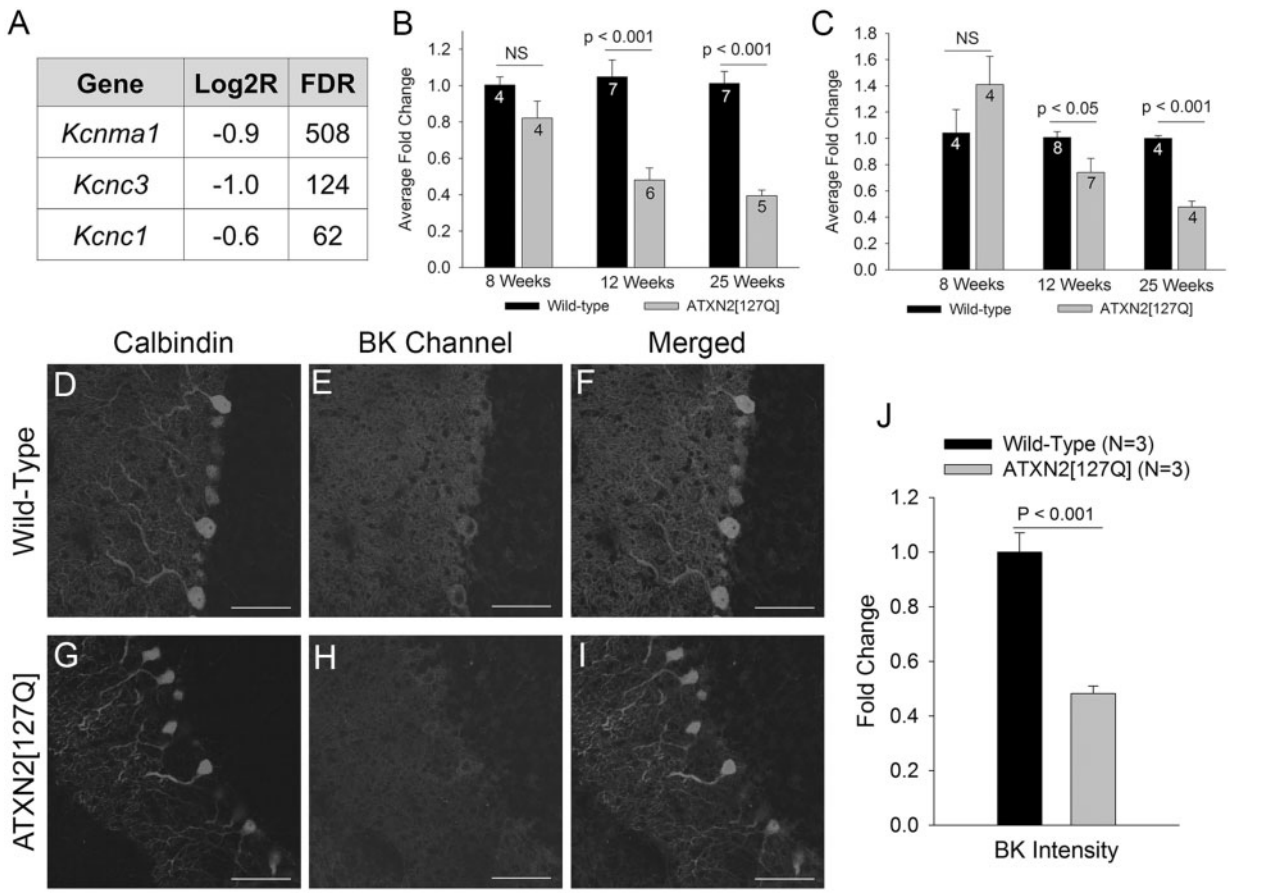

Figure 3. A progressive reduction in potassium channel transcripts accompanies degeneration in ATXN2[127Q] Purkinje neurons. (**A**) RNA sequencing from 6-week-old cerebella of ATXN2[127Q] mice and littermate controls reveals a reduction in transcripts of potassium channels important for Purkinje neuron spiking. FDR (false discovery rate) >30 corresponds to a corrected p value of < 0.01. (**B**) Quantitative RT-PCR for *Kcnma1* (BK) demonstrates a progressive reduction in BK channel transcripts in ATXN2[127Q] cerebella. (**C**) Quantitative RT-PCR for *Kcnc3* (Kv3.3) demonstrates a progressive reduction in Kv3.3 channel transcripts in ATXN2[127Q] cerebella. Immunostaining for calbindin (**D**) and BK channels (**E**) in wild-type Purkinje neurons shows prominent overlap of BK and calbindin staining (**F**). (**G**) In 25-week-old ATXN2[127Q] cerebella, calbindin immunostaining reveals prominent Purkinje neuron dendritic atrophy, with thinning of the molecular layer. (**H**) BK staining is reduced in ATXN2[127Q] Purkinje neurons, also seen in the merged image of BK and calbindin in (**I**) and summarized in (**J**). Data were analysed with a Student's *t*-test, and are displayed as mean ± SEM.

BK channels in wild-type neurons using iberiotoxin, a selective BK channel inhibitor. Iberiotoxin increased the firing frequency of wild-type Purkinje neurons, without causing spiking irregularities or bursting (Fig. 6A–C). In ATXN2[127Q] Purkinje neurons, surprisingly, Iberiotoxin caused irregular spiking with short bursts containing one to two spikelets (Fig. 6D–G). Iberiotoxin increased the overall firing frequency (Fig. 6H), but this effect disappeared when spikelets in doublets/spike bursts were excluded, so that the overall firing frequency was unchanged (Fig. 6I). Since iberiotoxin insensitive BK channels are reported to contribute to the AHP (21), we also determined the effect of 10 μM paxilline, which blocks both iberiotoxin-sensitive and insensitive BK currents (21). The effect of paxilline on firing was similar to that of iberiotoxin, with regular firing converted into spike bursts. Also, similar to iberiotoxin, when doublets and spikelets in bursts were excluded, there was no significant change in firing frequency ($n = 5$ cells, 25.2 ± 9.2 Hz before paxilline, and 20.3 ± 9.2 Hz following paxilline). These results suggest that in spite of the fact that BK channel transcripts and immunostaining is significantly reduced in ATXN2[127Q] Purkinje neurons, these neurons continue to depend on the BK channel mediated AHP to generate tonic, repetitive, regular spiking. The reduction in firing frequency and therefore the novel AHP in ATXN2[127Q] Purkinje neurons is not, however, mediated through BK channels.

The reduction in firing frequency in atrophic ATXN2[127Q] Purkinje neurons is secondary to a novel AHP generated by K_{ir} channels

The other calcium-activated potassium channel normally involved in regulating spiking and the AHP in Purkinje neurons is the SK channel. Apamin, a selective SK channel inhibitor increased firing frequency by only ~3 Hz in ATXN2[127Q] Purkinje neurons (Fig. 7A). This suggested that the reduced firing frequency, and the novel AHP in ATXN2[127Q] Purkinje neurons is due to a potassium current that does not normally play a significant role in Purkinje neuron spiking. In our studies in a model of SCA1, barium-sensitive subthreshold-activated, inwardly-rectifying potassium (K_{ir}) channels play an important role in maintaining spiking in atrophic Purkinje neurons (10). In order to determine whether K_{ir} channels may be playing a role in regulating spiking in atrophic ATXN2[127Q] Purkinje neurons we used 50 μM extracellular barium, which is selective for K_{ir} channels (22–25). Barium only had a modest effect on the firing

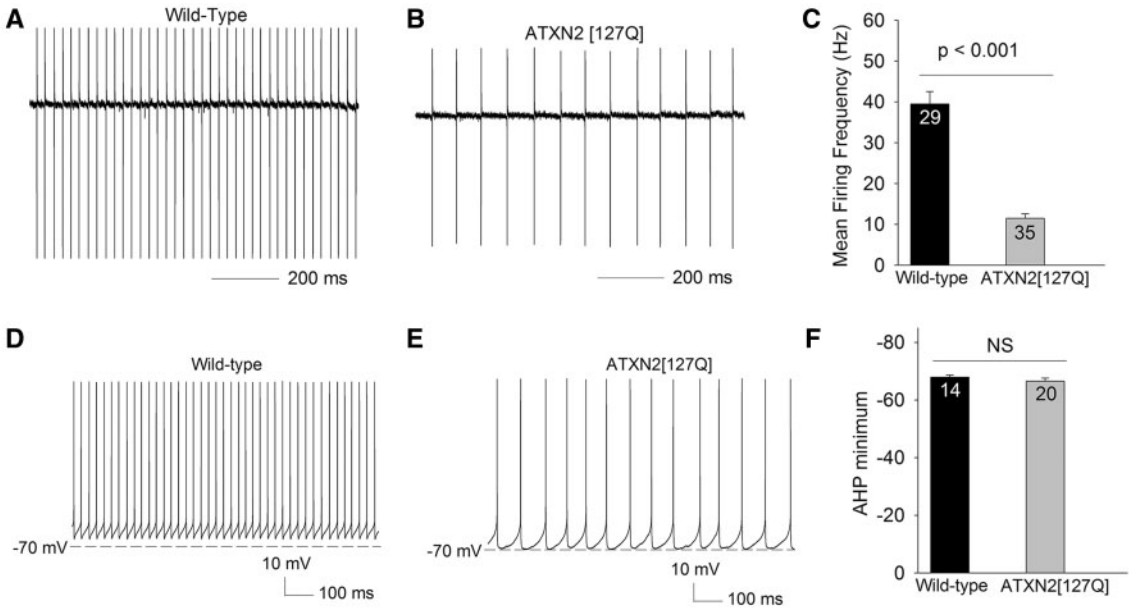

Figure 4. Atrophic 25-week ATXN2[127Q] Purkinje neurons are able to restore spiking in association with a normal AHP amplitude. (**A**) In the cell-attached configuration, wild-type Purkinje neurons at 25 weeks continue to display tonic repetitive spiking. (**B**) ATXN2[127Q] Purkinje neurons also display tonic repetitive spiking at 25 weeks, although at a greatly reduced firing frequency, summarized in (**C**). (**D**) In the whole-cell configuration wild-type Purkinje neurons display spikes with a prominent AHP. (**E**) ATXN2[127Q] Purkinje neurons display repetitive spiking with a similar amplitude AHP, summarized in (**F**). Data were analysed with a Student's *t*-test, and are displayed as mean ± SEM.

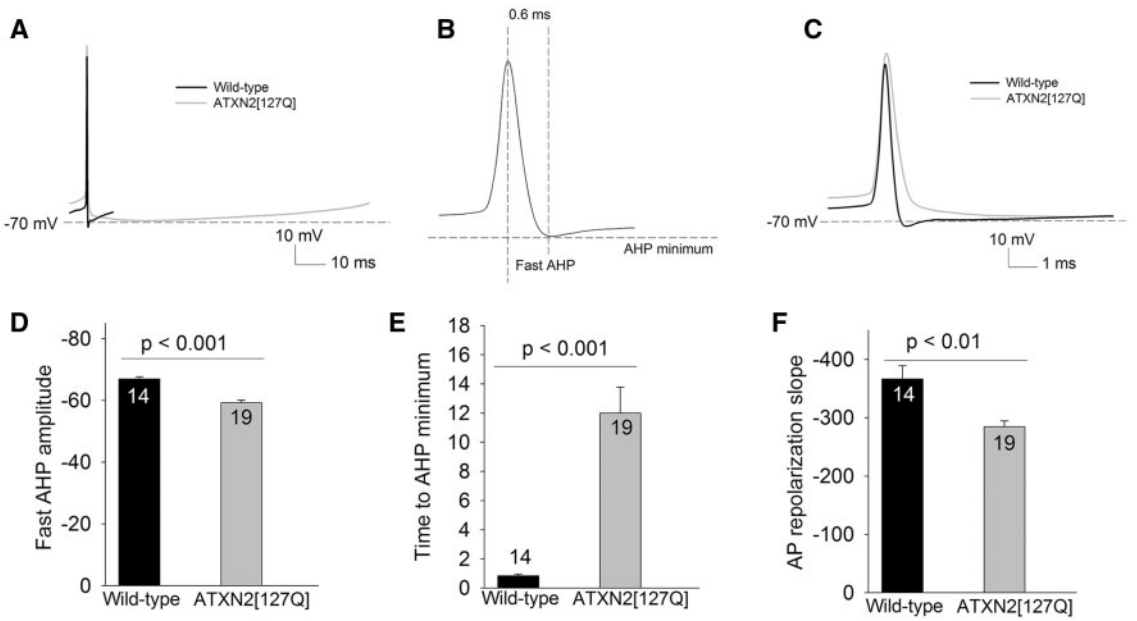

Figure 5. 25-week ATXN2[127Q] Purkinje neurons generate an AHP with novel kinetics. (**A**) Overlay of one interspike interval from a wild-type and ATXN2[127Q] Purkinje neuron showing a similar AHP amplitude. (**B**) Schematic action potential showing the location of the fast AHP and the AHP minimum. (**C**) Overlay of a spontaneous spike from a wild-type and ATXN2[127Q] Purkinje neuron on an expanded timescale to demonstrate the slowing of spike repolarization and reduced fast AHP amplitude in ATXN2[127Q] Purkinje neurons. (**D**) Summary of the fast AHP amplitude in ATXN2[127Q] Purkinje neurons. (**E**) The AHP minimum is delayed in ATXN2[127Q] Purkinje neurons. (**F**) The repolarization of the action potential (AP) is impaired in ATXN2[127Q] Purkinje neurons. Data were analysed with a Student's *t*-test, and are displayed as mean ± SEM.

frequency of wild-type neurons (Fig. 7B and D). Remarkably, barium normalized firing frequency of 25-week- old atrophic ATXN2[127Q] Purkinje neurons (Fig. 7C and D). Corresponding to the changes in firing frequency, in wild-type Purkinje neurons, barium had only a modest effect on the AHP amplitude (Fig. 7E and G). Barium had a large effect on reducing the AHP amplitude in ATXN2[127Q] Purkinje neurons (Fig. 7F and G). Significantly, the barium sensitive current contributes to the entire duration of the AHP, so that the time to AHP minimum is not altered in the presence of barium (Fig. 7G). No consistent changes were observed in K_{ir} channel transcripts and transcript levels of $GABA_B$ receptors (26), which indirectly activate

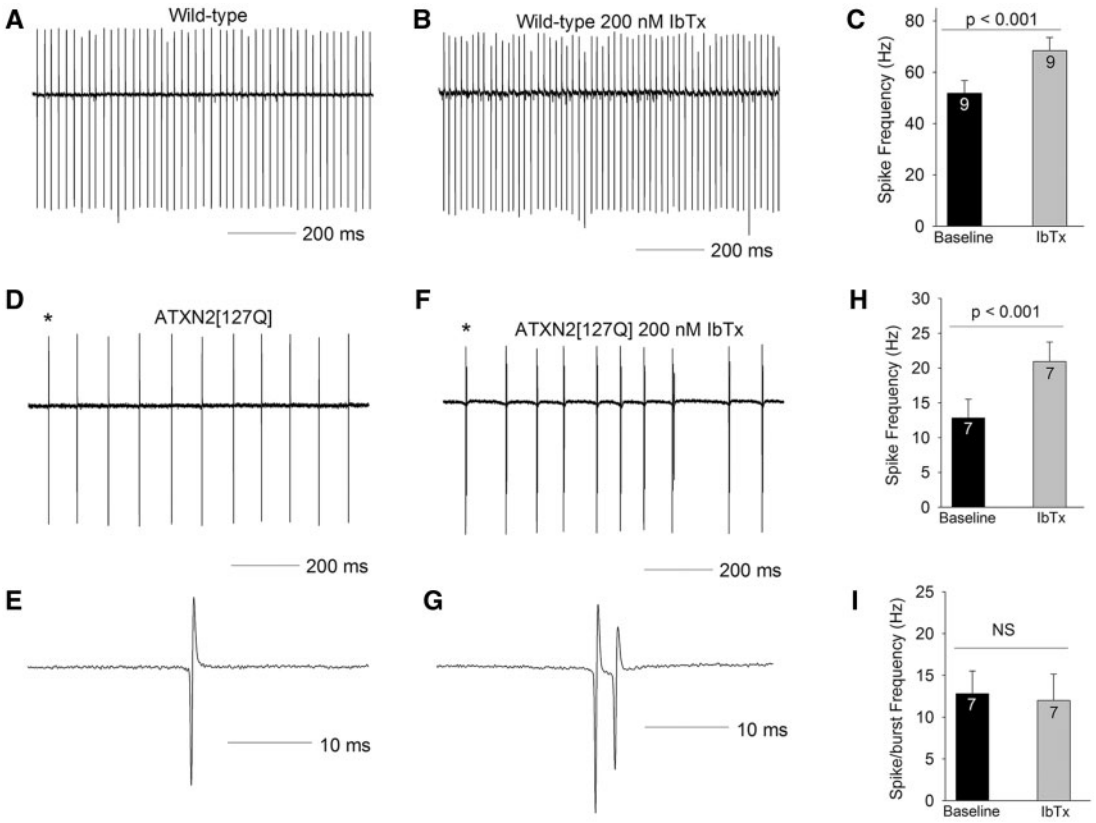

Figure 6. BK channels are not responsible for the slow firing in 25-week ATXN2[127Q] Purkinje neurons. (**A**) In the cell-attached configuration, wild-type Purkinje neurons at 25 weeks continue to display tonic repetitive spiking. (**B**) In this cell 200 nM iberiotoxin (IbTx) increases firing frequency, summarized in (**C**). (**D**) ATXN2[127Q] Purkinje neurons display tonic repetitive spiking at 25 weeks at a reduced firing frequency. (**E**) A single spike corresponding to the asterisk is shown on an expanded timescale. (**F**) In this cell, 200 nM iberiotoxin converts tonic spiking into tonic bursting, with each burst containing a spike followed by one or two spikelets. (**G**) A single spike-burst corresponding to the asterisk is shown on an expanded timescale, showing a spike and a spikelet. (**H**) Iberiotoxin increases firing frequency by converting spikes into spike-bursts. (**I**) Burst frequency is similar to the firing frequency of tonic repetitive spiking in the absence of iberiotoxin. Data were analysed with a Student's *t*-test, and are displayed as mean ± SEM.

K_{ir} channels, are reduced, suggesting that the increased activity of K_{ir} channels is not explained by alterations in the expression of these channels (Supplementary Material, Table S1). These results suggest that increased activity of K_{ir} channels is responsible for generating a novel AHP in atrophic ATXN2[127Q] Purkinje neurons, that causes a reduction in firing frequency.

Discussion

Purkinje neurons maintain repetitive spiking through the interplay of currents mediated by depolarizing voltage-gated sodium channels, and rapidly deactivating voltage-gated and calcium-activated potassium channels. The AHP, normally mediated by BK (16) and SK channels (16,17), also decays rapidly so that little potassium current is present in the interspike interval (1). In other neurons, distinct potassium channels mediate an AHP with slower kinetics. For example, a potassium channel distinct from SK and BK channels, mediates a slow AHP in the interspike interval of cortical neurons that do not exhibit autonomous pacemaking (27). K_{ir} channels support repetitive spiking at a relatively low frequency in pacemaker nociceptive neurons in the spinal cord (28). In ATXN2[127Q] Purkinje neurons, we demonstrate that in spite of a reduction in the BK channel mediated AHP, the overall amplitude of the AHP is maintained at a disease stage when there is significant Purkinje neuron atrophy. The kinetics and pharmacology of this AHP is similar to that of slow-firing pacemakers such as spinal cord nociceptive neurons (28). The exact mechanism for the generation of this novel barium sensitive AHP in ATXN2[127Q] Purkinje neurons is unclear, but may be secondary to the increased density of subthreshold activated potassium currents resulting from a reduction in cell size. The exact molecular identity of this subthreshold activated potassium channel is also unclear. Although both *Kcnj* (K_{ir} channels) (22–25,29) and some *Kcnk* (K2P channels) (30,31) are sensitive to external barium, K2P channels are an order of magnitude less sensitive to external barium (in the hundreds of μM) (30,31) than Kcnj channels (< 50 μM) (22–25,29). Since in our current study, 50 μM external barium had a profound effect on firing in ATXN2[127Q] Purkinje neurons, this is most consistent with a potassium current carried by K_{ir} channels. The exact identity of the channel will be difficult to identify due to the lack of availability of specific pharmacologic agents for these channels. K_{ir} channels are normally present in Purkinje neurons (10,32) but do not play a major role in controlling spike frequency or the AHP (1). In this study, we too demonstrate that low doses of extracellular barium, selective for K_{ir} channels (22–25), has a limited effect on firing frequency and the AHP in wild-type Purkinje neurons. In association with a reduction in Purkinje neuron size in SCA2, retained expression of subthreshold-activated potassium channels and correspondingly an increase in channel density, may allow for these channels to play an unusual role in

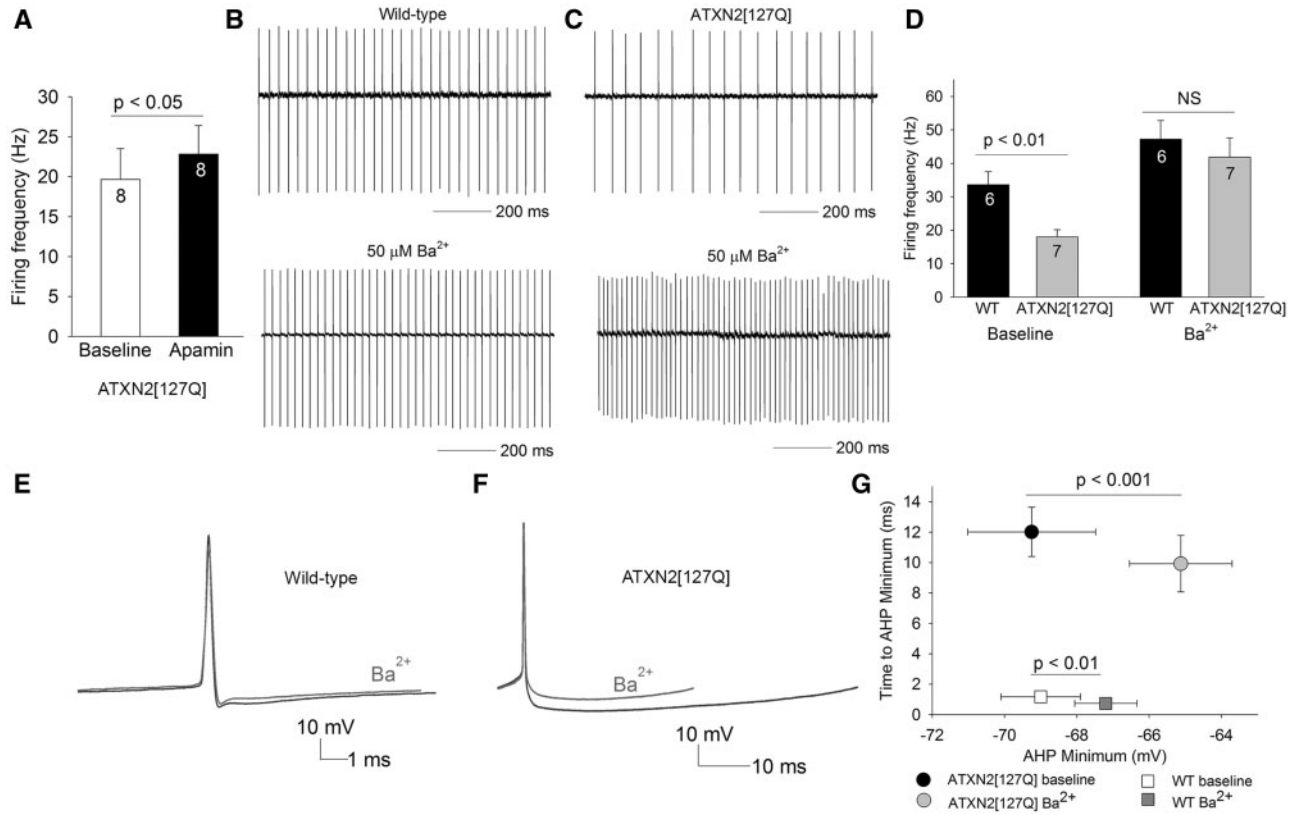

Figure 7. The novel AHP generated by K_{ir} channels is responsible for the reduced firing frequency of 25-week ATXN2[127Q] Purkinje neurons. (**A**) Apamin (100 nM) has a minimal effect on firing frequency of ATXN2[127Q] Purkinje neurons. (**B**) Wild-type neurons that display tonic repetitive spiking (top) have a modest increase in firing frequency in the presence of 50 μM extracellular barium. (**C**) ATXN2[127Q] Purkinje neurons (top) increase their firing frequency to wild-type levels in the presence of 50 μM extracellular barium, summarized in (**D**). (**E**) Barium has a modest effect on the AHP in wild-type Purkinje neurons ($n = 6$). (**F**) The barium sensitive current contributes the entire AHP in ATXN2[127Q] Purkinje neurons ($n = 8$), summarized in **G**. Data were analysed with a Student's *t*-test, and are displayed as mean ± SEM.

generating the AHP. It is interesting to speculate as to whether the increase in density of these channels is a homeostatic response in Purkinje neurons to retain repetitive spiking when channels (BK and Kv3.3) that usually play this role are no longer able to do so. A reduction in cell size of Purkinje neurons due the degenerative process thus makes them resemble other pacemaker neurons in both size, and in utilizing K_{ir} channels that are normally used by these other neurons for slower pacemaking. It is possible that a distinct repertoire of ion-channels is part of a cell-size associated program for pacemaking.

A reduction in Purkinje neuron firing frequency is a common feature of distinct ataxia causing channelopathies. Kv3.3 knockout mice, a model for SCA13 (33), have reduced spontaneous firing due to decreased availability of voltage-gated sodium channel resurgent-current in the interspike interval (15). Purkinje neurons in BK channel knockout mice also have reduced firing frequency secondary to reduced recovery of voltage-gated sodium channels from inactivation (18). Neither of these mouse models of ataxia, however, have changes in Purkinje neuron size or neurodegeneration. At 12 weeks, when there is little Purkinje neuron atrophy, and there is a reduction in BK and Kv3.3 transcripts, the reduction in firing frequency and membrane depolarization in ATXN2[127Q] Purkinje neurons is likely due to the loss of membrane repolarization mediated by these channels, and thus the inability of voltage-gated sodium channels to recover from inactivation. Although reduced transcript levels of both Kv3.3 and BK are more profound in ATXN2[127Q] mice at 25 weeks, when there is marked Purkinje neuron atrophy, the reduced Purkinje neuron firing frequency is due to a mechanism distinct from changes in voltage-gated sodium channel kinetics. Although there are functional consequences of reduced BK and Kv3.3 channels in Purkinje neuron spiking, atrophic SCA2 Purkinje neurons are able to hyperpolarize the membrane sufficiently through a novel K_{ir} current mediated mechanism. In SCA1 mice, which also display reduced Purkinje neuron firing frequency, a reduction in BK and subthreshold-activated potassium channels contributes to Purkinje neuron atrophy. A reduction in Purkinje cell size in a mouse model of SCA1 is able to increase BK channel density, so that these channels not only continue to play a major role in repetitive spiking (10), but also generate a normal amplitude fast AHP. Although changes in membrane excitability resulting from a reduction of Kv3.3 and BK channels may contribute similarly to Purkinje neuron atrophy in SCA2, cell atrophy does not increase the density of BK channels sufficiently in ATXN2[127Q] Purkinje neurons to enable BK channels to continue to generate a normal amplitude fast-AHP. Nevertheless, BK channels play an important role in enabling atrophic ATXN2[127Q] Purkinje neurons to maintain discrete spikes, and preventing spike doublets/bursts. The importance of BK channels in maintaining normal firing frequency in atrophic ATXN2[127Q] Purkinje neurons is however greatly diminished. The reduction in firing frequency in atrophic SCA2 Purkinje neurons is therefore independent of the reduced activity of BK and Kv3.3 channels.

Alterations in Purkinje neuron spiking are associated with motor dysfunction in a variety of mouse models of ataxia (6,34).

Normalizing Purkinje neuron spiking is associated with improved motor function in mouse models (34,35). In these studies, the target for improvement in Purkinje neuron spiking has primarily been calcium-activated potassium channels (6,35). The utility of calcium-activated potassium channel activators in improving motor dysfunction is also established in a different model of SCA2, where there is not prominent Purkinje neuron atrophy (36). The calcium-activated potassium channels, BK and SK, normally play a vital role in Purkinje neuron repetitive spiking, and disruption of calcium-activated potassium channel function results in ataxia (18,37,38). In this study, we demonstrate that prior to substantial Purkinje neuron atrophy in SCA2, early in the disease process, there is a reduction of BK and Kv3.3 channel expression and function. In Purkinje neurons, since BK channel function is closely tied to calcium entry, the net effect of calcium entry is activation of calcium-activated potassium channels (1). We cannot therefore rule out the possibility that dysfunction of voltage-gated calcium channels, in addition to reduced BK channel transcripts, also contributes to reduced BK channel function. In any event, reduced BK and Kv3.3 channel function is associated with disrupted Purkinje neuron spiking and membrane depolarization in a fashion similar to mice with a knockout of the respective channels. With the onset of Purkinje neuron atrophy, however, although BK channels continue to play a role in supporting spiking, Purkinje neurons rely on K_{ir} channels to maintain a normal AHP amplitude. Activating potassium channels at this stage of disease is likely to have either no effect on spiking, or a further slowing of firing frequency and would therefore likely either not improve, or worsen motor function. If a similar pattern of changes in Purkinje neuron physiology occurs in human cerebellar ataxia, it would be important to consider the stage in the disease process before considering potassium channel activators to treat motor symptoms.

Materials and Methods

Mice

All animal procedures were approved by the University of Michigan Committee on the Use and Care of Animals. The ATXN2[127Q] transgenic mice overexpress mutant human ATXN2 with 127 CAG repeats selectively in cerebellar Purkinje neurons under the *Pcp2 (L7)* promoter as described previously (11). Hemizygous ATXN2[127Q] mice and wild-type littermate controls were used in all experiments. Mice used for these experiments were between 12 and 25 weeks old. Mice of both sexes were used for all experiments.

Immunofluorescence

Mice were anesthetized with isoflurane and brains were removed, fixed in 1% paraformaldehyde for 1 h, immersed in 30% sucrose in PBS and sectioned on a CM1850 cryostat (Leica). 14 μm parasagittal sections were processed for immunohistochemistry. Purkinje cells were labeled with anti-calbindin antibody (Swant 1:1000 (Marly, Switzerland), or Cell Signaling Technologies 1:200 (Danvers, MA)) and an appropriate secondary goat anti-mouse Alexa Fluor antibody (Life Technologies Molecular Probes, Grand Island, NY). Sections were imaged using a FV500 Olympus Confocal Microscope and single plane images were obtained. Measurements of molecular layer thickness were made for each section, 100 μm from the depth of the primary fissure as previously described (10). Dual calbindin (rabbit, 1: 200, Cell signaling Technologies, Beverly, MA) and BK channel (1:500, Clone L6/60, mouse monoclonal antibodies were obtained from the UC Davis/NIH NeuroMab facility) immunostaining was performed. Measurement of staining intensity was performed in the cerebellar molecular layer. In order to eliminate selection bias, an area of strong calbindin staining was identified for each image, and the corresponding region was analysed for BK staining. Average staining intensity was measured in a circle of uniform area in each image. Approximately 30 images were analysed for each genotype at each time point. The intensity values were averaged by age and genotype. Sample preparation was performed and images were obtained with experimenter blind to genotype.

RNA isolation and quantitative real-time PCR

Mice were euthanized following anesthesia with isoflurane, and cerebella were removed and flash-frozen in liquid nitrogen. Tissue was stored at −80 °C until the time of processing. Total RNA from each harvested mouse cerebellum was extracted using Trizol Reagent (Invitrogen) and subsequently purified using the RNeasy mini kit (Qiagen) following the manufacturer's instructions. cDNA was synthesized from 1 μg of purified RNA using the iScript cDNA synthesis kit (Cat. no. 1708891, Bio-Rad). Quantitative real-time PCR assays were performed using the iQ SYBR Green Supermix (Cat. no. 1708880, Bio-Rad) in a MyiQ Single Color Real-Time PCR Detection System (Bio-Rad), with each reaction performed at a 20 μl sample volume in an iCycler iQ PCR 96-well Plate (Bio-Rad) sealed with Microseal optical sealing tape (Bio-Rad). The relative amount of transcript mRNA was determined using the comparative C_t method for quantitation (39) with *Actb* mRNA serving as the reference gene. C_t values for each sample were obtained in triplicate and averaged for statistical comparisons. The primers used for qRT-PCR are listed as follows: (1) *Kcnma1* (Forward: AGC CAA CGA TAA GCT GTG GT), (Reverse: AAT CTC AAG CCA AGC CAA CT), (2) *Kcnc3* (Forward: TTG AGG ACC CCT ACT CGT C), (Reverse: CTG ATG TGG ATG AAG CCC TC) and (3) *Actb* (Forward: CGG TTC CGA TGC CCT GAG GCT CTT), (Reverse: CGT CAC ACT TCA TGA TGG AAT TGA).

RNA sequencing. Cerebella from 6-week-old ATXN2[127Q] and wild-type littermates (16 animals in each group) were used for RNA sequence analyses. Total RNA was isolated using miRNeasy Mini Kit (Qiagen Inc., USA) according to the manufacturer's protocol. RNA quality was determined using the Bioanalyzer 2100 Pico Chip (Agilent). Samples with an RNA integrity number (RIN) >8 were used for library preparation using Illumina TrueSeq Stranded Total RNA Sample Prep with Ribo-Zero rRNA Removal Kit for mouse. Single-end 50-bp reads were generated on a Hiseq 2000 sequencing machine at the University of Utah Microarray and Genomic Analysis Shared Resource using Illumina Version 4 flow cells. Reads were then aligned to the mouse reference genome (mm10) by Novoalign (http://www.novocraft.com) as previously described (19).

Preparation of brain slices for electrophysiological recordings. Mice were anesthetized by isofluorane inhalation, decapitated, and the brains were chilled in ice-cold cutting solution containing (in mM): 87 NaCl, 2.5 KCl, 25 $NaHCO_3$, 1 NaH_2PO_4, 0.5 $CaCl_2$, 7 $MgCl_2$, 75 sucrose and 10 glucose, bubbled with 5% CO_2/95% O_2. 300 μm parasagittal cerebellar slices were cut using a vibratome. Slices were incubated at 33 °C in artificial CSF (ACSF) containing (in mM): 125 NaCl, 3.5 KCl, 26 $NaHCO_3$, 1.25 NaH_2PO_4, 2 $CaCl_2$, 1 $MgCl_2$ and 10 glucose, bubbled with 5% CO_2 + 95% O_2 (carbogen) for 45 min. Slices were stored at room temperature until use.

Slices were then placed in a recording chamber and continuously perfused with carbogen-bubbled ACSF at 33 °C with a flow rate of 2–3 ml/min.

Whole-cell recordings. Purkinje neurons were identified for patch-clamp recordings in parasagittal cerebellar slices. Borosilicate glass patch pipettes (with resistances of 2–4 MΩ) were filled with internal recording solution containing (in mM): 119 K Gluconate, 2 Na Gluconate, 6 NaCl, 2 $MgCl_2$, 0.9 EGTA, 10 HEPES, 14 Tris-Phosphocreatine, 4 MgATP, 0.3 tris-GTP, pH 7.3. Whole-cell recordings at 33 °C were made in ACSF 1–5 h after slice preparation using an Axopatch 200B amplifier, Digidata 1440 A interface and pClamp-10 software (MDS analytical technologies, Sunnyvale, CA) as previously described. Voltage data were acquired in the fast current clamp mode of the amplifier and filtered at 2 kHz. Cells were rejected if the series resistance changed by greater than 20% in the course of the recording or if it exceeded 15 MΩ. Data were digitized at 100 kHz. Voltage traces were corrected for a 10 mV liquid junction potential. In order to determine the effect of pharmacologic agents on firing, agents were perfused on slices for at least 8 min or until changes in firing reached equilibrium. The coefficient of variation (CV) was calculated as the ratio of the standard deviation of the interspike interval divided by the mean interspike interval. In order to prevent inaccuracies due to changes in threshold of spiking, the absolute value of the membrane potential was recorded as the AHP at specified time points following the peak of the spike. The spike threshold was defined as 10% of the maximum slope of the rising phase of the action potential. In order to calculate depolarization and repolarization slopes, the 1st order differential of either the upward or downward deflection of the action potential was calculated, and the respective most positive or negative value is reported.

Statistical analysis

Statistical significance for electrophysiology was assessed by either an unpaired Student's *t*-test, Fisher's exact test. A paired Student's *t*-test was used to determine the effect of pharmacologic agents on firing properties. Data were considered significant for $P < 0.05$. Data are expressed as mean ± SEM unless otherwise specified. Data were analysed using SigmaPlot (Systat Software Inc), GraphPad Prism (GraphPad Software Inc.) and Excel (Microsoft Corp).

Supplementary Material

Supplementary Material is available at *HMG* online.

Acknowledgements

We thank John Cooper, Brandon Lee, Annie Zalon, Alexi Vasbinder, and Allison Sylvia for technical support. We thank Ravi Chopra for helpful comments and suggestions.

Conflict of Interest statement. None declared.

Funding

National Institute of Neurological Disorders and Stroke (NINDS), NIH R01NS085054 (V.G.S.).

References

1. Raman, I.M. and Bean, B.P. (1999) Ionic currents underlying spontaneous action potentials in isolated cerebellar Purkinje neurons. *J. Neurosci.*, **19**, 1663–1674.
2. Hausser, M. and Clark, B.A. (1997) Tonic synaptic inhibition modulates neuronal output pattern and spatiotemporal synaptic integration. *Neuron*, **19**, 665–678.
3. Bell, C.C. and Grimm, R.J. (1969) Discharge properties of Purkinje cells recorded on single and double microelectrodes. *J. Neurophysiol.*, **32**, 1044–1055.
4. Thach, W.T. (1968) Discharge of Purkinje and cerebellar nuclear neurons during rapidly alternating arm movements in the monkey. *J. Neurophysiol.*, **31**, 785–797.
5. Thach, W.T. (1978) Correlation of neural discharge with pattern and force of muscular activity, joint position, and direction of intended next movement in motor cortex and cerebellum. *J. Neurophysiol.*, **41**, 654–676.
6. Chopra, R. and Shakkottai, V.G. (2014) Translating cerebellar Purkinje neuron physiology to progress in dominantly inherited ataxia. *Future Neurol.*, **9**, 187–196.
7. De Zeeuw, C.I., Hoebeek, F.E., Bosman, L.W., Schonewille, M., Witter, L. and Koekkoek, S.K. (2011) Spatiotemporal firing patterns in the cerebellum. *Nat. Rev. Neurosci.*, **12**, 327–344.
8. Shakkottai, V.G. and Fogel, B.L. (2013) Clinical neurogenetics: autosomal dominant spinocerebellar ataxia. *Neurol. Clin.*, **31**, 987–1007.
9. Hourez, R., Servais, L., Orduz, D., Gall, D., Millard, I., de Kerchove d'Exaerde, A., Cheron, G., Orr, H.T., Pandolfo, M. and Schiffmann, S.N. (2011) Aminopyridines correct early dysfunction and delay neurodegeneration in a mouse model of spinocerebellar ataxia type 1. *J. Neurosci.*, **31**, 11795–11807.
10. Dell'Orco, J.M., Wasserman, A.H., Chopra, R., Ingram, M.A., Hu, Y.S., Singh, V., Wulff, H., Opal, P., Orr, H.T. and Shakkottai, V.G. (2015) Neuronal Atrophy Early in Degenerative Ataxia Is a Compensatory Mechanism to Regulate Membrane Excitability. *J. Neurosci.*, **35**, 11292–11307.
11. Hansen, S.T., Meera, P., Otis, T.S. and Pulst, S.M. (2013) Changes in Purkinje cell firing and gene expression precede behavioral pathology in a mouse model of SCA2. *Hum. Mol. Genet.*, **22**, 271–283.
12. Shakkottai, V.G., do Carmo Costa, M., Dell'Orco, J.M., Sankaranarayanan, A., Wulff, H. and Paulson, H.L. (2011) Early changes in cerebellar physiology accompany motor dysfunction in the polyglutamine disease spinocerebellar ataxia type 3. *J. Neurosci.*, **31**, 13002–13014.
13. Perkins, E.M., Clarkson, Y.L., Sabatier, N., Longhurst, D.M., Millward, C.P., Jack, J., Toraiwa, J., Watanabe, M., Rothstein, J.D., Lyndon, A.R. *et al.* (2010) Loss of beta-III spectrin leads to Purkinje cell dysfunction recapitulating the behavior and neuropathology of spinocerebellar ataxia type 5 in humans. *J. Neurosci.*, **30**, 4857–4867.
14. Shakkottai, V.G., Xiao, M., Xu, L., Wong, M., Nerbonne, J.M., Ornitz, D.M. and Yamada, K.A. (2009) FGF14 regulates the intrinsic excitability of cerebellar Purkinje neurons. *Neurobiol. Dis.*, **33**, 81–88.
15. Akemann, W. and Knopfel, T. (2006) Interaction of Kv3 potassium channels and resurgent sodium current influences the rate of spontaneous firing of Purkinje neurons. *J. Neurosci.*, **26**, 4602–4612.
16. Edgerton, J.R. and Reinhart, P.H. (2003) Distinct contributions of small and large conductance Ca2+-activated K+ channels to rat Purkinje neuron function. *J. Physiol.*, **548**, 53–69.

17. Cingolani, L.A., Gymnopoulos, M., Boccaccio, A., Stocker, M. and Pedarzani, P. (2002) Developmental regulation of small-conductance Ca2+-activated K+ channel expression and function in rat Purkinje neurons. *J. Neurosci.*, **22**, 4456–4467.
18. Sausbier, M., Hu, H., Arntz, C., Feil, S., Kamm, S., Adelsberger, H., Sausbier, U., Sailer, C.A., Feil, R., Hofmann, F. *et al.* (2004) Cerebellar ataxia and Purkinje cell dysfunction caused by Ca2+-activated K+ channel deficiency. *Proc. Natl. Acad. Sci. U.S.A*, **101**, 9474–9478.
19. Dansithong, W., Paul, S., Figueroa, K.P., Rinehart, M.D., Wiest, S., Pflieger, L.T., Scoles, D.R. and Pulst, S.M. (2015) Ataxin-2 regulates RGS8 translation in a new BAC-SCA2 transgenic mouse model. *PLoS Genet.*, **11**, e1005182.
20. Chen, X., Kovalchuk, Y., Adelsberger, H., Henning, H.A., Sausbier, M., Wietzorrek, G., Ruth, P., Yarom, Y. and Konnerth, A. (2010) Disruption of the olivo-cerebellar circuit by Purkinje neuron-specific ablation of BK channels. *Proc. Natl. Acad. Sci. U.S.A*, **107**, 12323–12328.
21. Benton, M.D., Lewis, A.H., Bant, J.S. and Raman, I.M. (2013) Iberiotoxin-sensitive and -insensitive BK currents in Purkinje neuron somata. *J. Neurophysiol.*, **109**, 2528–2541.
22. Quayle, J.M., McCarron, J.G., Brayden, J.E. and Nelson, M.T. (1993) Inward rectifier K+ currents in smooth muscle cells from rat resistance-sized cerebral arteries. *Am. J. Physiol.*, **265**, C1363–C1370.
23. Franchini, L., Levi, G. and Visentin, S. (2004) Inwardly rectifying K+ channels influence Ca2+ entry due to nucleotide receptor activation in microglia. *Cell Calcium*, **35**, 449–459.
24. Hibino, H., Inanobe, A., Furutani, K., Murakami, S., Findlay, I. and Kurachi, Y. (2010) Inwardly rectifying potassium channels: their structure, function, and physiological roles. *Physiol. Rev.*, **90**, 291–366.
25. Sepulveda, F.V., Pablo Cid, L., Teulon, J. and Niemeyer, M.I. (2015) Molecular aspects of structure, gating, and physiology of pH-sensitive background K2P and Kir K+-transport channels. *Physiol. Rev.*, **95**, 179–217.
26. Pflieger, L.T., Dansithong, W., Paul, S., Scoles, D., Figueroa, K.P., Meera, P., Otis, T.S., Facelli, J.C. and Pulst, S.M. (2017) Gene co-expression network analysis for identifying modules and functionally enriched pathways in SCA2. *Hum. Mol. Genet.*, **26**, 3069–3080.
27. Villalobos, C., Shakkottai, V.G., Chandy, K.G., Michelhaugh, S.K. and Andrade, R. (2004) SKCa channels mediate the medium but not the slow calcium-activated afterhyperpolarization in cortical neurons. *J. Neurosci.*, **24**, 3537–3542.
28. Li, J., Blankenship, M.L. and Baccei, M.L. (2013) Inward-rectifying potassium (Kir) channels regulate pacemaker activity in spinal nociceptive circuits during early life. *J. Neurosci.*, **33**, 3352–3362.
29. Alagem, N., Dvir, M. and Reuveny, E. (2001) Mechanism of Ba(2+) block of a mouse inwardly rectifying K+ channel: differential contribution by two discrete residues. *J. Physiol.*, **534**, 381–393.
30. Ma, X.Y., Yu, J.M., Zhang, S.Z., Liu, X.Y., Wu, B.H., Wei, X.L., Yan, J.Q., Sun, H.L., Yan, H.T. and Zheng, J.Q. (2011) External Ba2+ block of the two-pore domain potassium channel TREK-1 defines conformational transition in its selectivity filter. *J. Biol. Chem.*, **286**, 39813–39822.
31. O'Connell, A.D., Morton, M.J., Sivaprasadarao, A. and Hunter, M. (2005) Selectivity and interactions of Ba2+ and Cs+ with wild-type and mutant TASK1 K+ channels expressed in Xenopus oocytes. *J. Physiol.*, **562**, 687–696.
32. Bushell, T., Clarke, C., Mathie, A. and Robertson, B. (2002) Pharmacological characterization of a non-inactivating outward current observed in mouse cerebellar Purkinje neurones. *Br. J. Pharmacol.*, **135**, 705–712.
33. Waters, M.F., Minassian, N.A., Stevanin, G., Figueroa, K.P., Bannister, J.P., Nolte, D., Mock, A.F., Evidente, V.G., Fee, D.B., Muller, U. *et al.* (2006) Mutations in voltage-gated potassium channel KCNC3 cause degenerative and developmental central nervous system phenotypes. *Nat. Genet.*, **38**, 447–451.
34. Chopra, R. and Shakkottai, V.G. (2014) The role for alterations in neuronal activity in the pathogenesis of polyglutamine repeat disorders. *Neurotherapeutics*, **11**, 751–763.
35. Bushart, D.D., Murphy, G.G. and Shakkottai, V.G. (2016) Precision medicine in spinocerebellar ataxias: treatment based on common mechanisms of disease. *Ann. Transl. Med.*, **4**, 25.
36. Kasumu, A.W., Hougaard, C., Rode, F., Jacobsen, T.A., Sabatier, J.M., Eriksen, B.L., Strobaek, D., Liang, X., Egorova, P., Vorontsova, D. *et al.* (2012) Selective positive modulator of calcium-activated potassium channels exerts beneficial effects in a mouse model of spinocerebellar ataxia type 2. *Chem. Biol.*, **19**, 1340–1353.
37. Walter, J.T., Alvina, K., Womack, M.D., Chevez, C. and Khodakhah, K. (2006) Decreases in the precision of Purkinje cell pacemaking cause cerebellar dysfunction and ataxia. *Nat. Neurosci.*, **9**, 389–397.
38. Shakkottai, V.G., Chou, C.H., Oddo, S., Sailer, C.A., Knaus, H.G., Gutman, G.A., Barish, M.E., LaFerla, F.M. and Chandy, K.G. (2004) Enhanced neuronal excitability in the absence of neurodegeneration induces cerebellar ataxia. *J. Clin. Invest.*, **113**, 582–590.
39. Livak, K.J. and Schmittgen, T.D. (2001) Analysis of relative gene expression data using real-time quantitative PCR and the 2(-Delta Delta C(T)) Method. *Methods*, **25**, 402–408.